

RESEARCH ARTICLE | MARCH 02 2023

# Effects of cobalt-permalloy cosputtering in a nanowire structure on magnetic fluctuation and auto-oscillation

Special Collection: [67th Annual Conference on Magnetism and Magnetic Materials](#)

ByungRo Kim ; S. Hwang; Seungha Yoon; S. H. Han; B. K. Cho  

 Check for updates

*AIP Advances* 13, 035107 (2023)  
<https://doi.org/10.1063/9.0000437>



**APL Electronic Devices**  
Open, quality research for the broad electronics community

## Meet the new Editor-in-Chief



[Learn More](#)

# Effects of cobalt-permalloy cosputtering in a nanowire structure on magnetic fluctuation and auto-oscillation

Cite as: AIP Advances 13, 035107 (2023); doi: 10.1063/9.0000437

Submitted: 2 October 2022 • Accepted: 25 December 2022 •

Published Online: 2 March 2023



View Online



Export Citation



CrossMark

ByungRo Kim,<sup>1,2</sup>  S. Hwang,<sup>1</sup> Seungha Yoon,<sup>2</sup> S. H. Han,<sup>3</sup> and B. K. Cho<sup>1,a)</sup> 

## AFFILIATIONS

<sup>1</sup>School of Materials Science and Engineering, Gwangju Institute of Science and Technology, 123 Cheomdangwagi-ro, Buk-gu, Gwangju 61005, South Korea

<sup>2</sup>Green Energy & Nano Technology R&D Group, Korea Institute of Industrial Technology, 6, Cheomdangwagi-ro 208-gil, Buk-gu, Gwangju 61012, South Korea

<sup>3</sup>Division of Navigation Science, Mokpo National Maritime University, Mokpo 58628, Republic of Korea

**Note:** This paper was presented at the 67th Annual Conference on Magnetism and Magnetic Materials.

**a)** Author to whom correspondence should be addressed: [chobk@gist.ac.kr](mailto:chobk@gist.ac.kr)

## ABSTRACT

A magnetic nanostructure for auto-oscillation, induced by spin-transfer torque, is fabricated by cosputtering permalloy with cobalt. Although the system does not meet the critical size and current requirements for direct auto-oscillation, magnetic signals resulting from spin wave excitation and magnetic fluctuations are measured by a Brillouin light scattering (BLS) system. From the analysis of the BLS spectrum, the threshold current for auto-oscillation is estimated to be 27.3% lower in  $\text{Py}_{1-x}\text{Co}_x$  ( $x = 0.2095$ ) than in  $\text{Py}_{1-x}\text{Co}_x$  ( $x = 0.0$ ). It is surmised that the cobalt in permalloy improves the efficiency of transferring spin torque for auto-oscillation.

© 2023 Author(s). All article content, except where otherwise noted, is licensed under a Creative Commons Attribution (CC BY) license (<http://creativecommons.org/licenses/by/4.0/>). <https://doi.org/10.1063/9.0000437>

## INTRODUCTION

Spin torque nano oscillators (STNOs) and spin Hall nano oscillators (SHNOs) are known as promising candidates for the excitation of propagating spin waves and as generators and detectors of ultra-tunable microwaves.<sup>1,2</sup> Unlike conventional devices based on semiconductors that utilize current flow for information processing, spin-based devices exploit electron spin to induce electric or magnetic signals. Recently, STNOs and SHNOs have been reportedly used as nonlinear oscillators in neuromorphic computing due to their benefits of long lifetimes, low-energy operation and scalability below the submicron size.<sup>3,4</sup>

STNOs are microwave generators that induce spin oscillation in a free layer using spin-transfer torque from a fixed layer. In such devices, the direct current, which flows through the nanostructure, inevitably causes damage because of electromigration and ohmic heating.<sup>5</sup> On the other hand, SHNOs utilize the spin-Hall effect in materials with strong spin-orbit coupling. The spin-Hall effect is a relativistic spin-orbit coupling phenomenon that induces an electric

charge current to generate a transverse spin current.<sup>3,6</sup> In the SHNO structure, current flows through a heavy metal layer underneath the free magnetic layer and induces spin current out of the heavy metal layer. SHNOs have several advantages over STNOs. For example, the structure of an SHNO is relatively simple, allowing for direct optical measurement using magneto-optical techniques.<sup>5,7</sup> In addition, because of their simple fabrication procedure, SHNO arrays can be synchronized easily for enhanced coherence.<sup>8–10</sup>

In general, current-induced spin torque in SHNOs plays a key role in anti-damping torque, which completely compensates for natural damping when auto-oscillations occur.<sup>7</sup> The threshold current density for auto oscillation is large compared to that of STNOs because of the low efficiency of charge-to-spin current conversion.<sup>11</sup> Thus, near the threshold current, additional damping due to scattering from nonlinear interactions between multiple modes emerges and prevents the ferromagnetic layer from the onset of auto-oscillation.<sup>12,13</sup> To avoid the nonlinear scattering process, several experiments have been performed in spatially confined structures. For example, a nanogap spin Hall oscillator achieves auto-oscillation

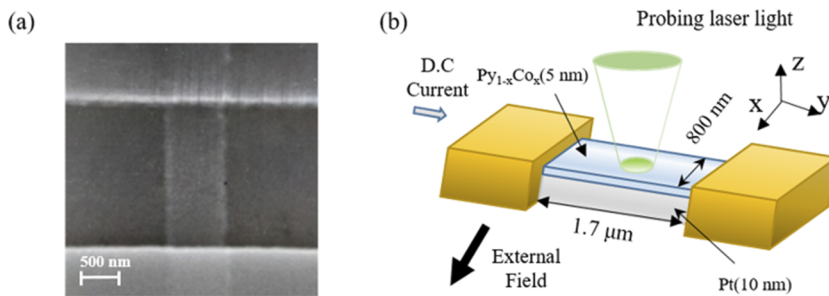


**FIG. 1.** (a) Scanning electron microscopy image of the top surface of the nanowire structure. (b) Schematic structure of stacked layers of Pt (10 nm)/Py<sub>1-x</sub>Co<sub>x</sub> (5 nm) and a contact pad. Configuration of the applied field and current is indicated by arrows, and the circular laser spot is focused on the center of the Py<sub>1-x</sub>Co<sub>x</sub> layer.

by selectively suppressing all modes except for a mode that auto-oscillates.<sup>12</sup> A nanoconstriction spin Hall oscillator achieved auto-oscillations by confining the potential well in its bow tie structure.<sup>7</sup> Such structures could prevent nonlinear scattering by minimizing the sample size to reduce the number of modes from the structure size.

Several studies have reported efforts to enhance the performance of STNOs or SHNOs, in which high output power, low phase noise and energy efficiency have been achieved. Divinskiy *et al.* showed an increase in oscillation amplitude by using a CoNi nanoconstriction structure with multilayer perpendicular magnetic anisotropy (PMA). Mohammad *et al.* demonstrated the enhancement of power density using the mutual synchronization of multiple nanoconstriction structures.<sup>14–18</sup> To reduce the threshold current in SHNOs, the heavy metal tungsten (W), instead of platinum (Pt), is used.<sup>19</sup> For effective charge-to-spin conversion, modulation of the thickness or interface of heavy metals is adopted by controlling the Pt thickness.<sup>20</sup>

Since the cosputtering different materials has advantages for alloy formation in terms of uniformity and mass production, several studies have utilized cosputtering.<sup>14–18</sup> One example is the significant enhancement of spin current transparency when Co is used as an interface layer between heavy metals and ferromagnetic films.<sup>21</sup> In addition, when transition metals are cosputtered with Py(NiFe) and Co, the Gilbert damping constant is found to increase.<sup>22</sup> Considering these results, it is worthwhile to study the effects of cosputtering Co with Py in SHNOs.

We investigated magnetic fluctuation effects in a Permalloy (Ni<sub>80</sub>Fe<sub>20</sub>) nanostructure, when it is cosputtered with Co, using micro-focused Brillouin light scattering spectroscopy ( $\mu$ -BLS). We observed that Co reduces the threshold current for the excitation of magnetic waves in SHNOs. In particular, for sputtering a stoichiometric ratio of Py<sub>0.7905</sub>Co<sub>0.2095</sub>, the nanowire structure shows a threshold current that is  $\sim 27.6\%$  lower than that of the pristine sample.

## EXPERIMENT

Figures 1(a) and 1(b) show scanning electron microscopy (SEM) image and schematic structure of a nanowire sample  $0.8 \mu\text{m}$  in width and  $2 \mu\text{m}$  in length. The nanowire consists of a layer stack, Ta(1)/Pt(10)/Py<sub>1-x</sub>Co<sub>x</sub>(5)/Al<sub>2</sub>O<sub>3</sub>(5), where the number is the thickness of each layer in units of nm. The nominal thickness of the layer is determined by the growth rate target and time in the sputtering

system. The Pt layer is used as a heavy metal for the generation of the spin Hall effect. The Py<sub>1-x</sub>Co<sub>x</sub> layer is fabricated by co sputtering Co and Py with stoichiometric ratios of  $x = 0, 0.1114, 0.2095, 0.2892$  and  $0.4030$ . The Ta and Al<sub>2</sub>O<sub>3</sub> layers are buffer layers above the substrate and capping layer, respectively. An AJA magnetron sputtering system with an initial base pressure of  $1 \times 10^{-9}$  Torr is used to fabricate samples without breaking vacuum in the whole process.

Since the  $\mu$ -BLS system can detect the excitation of spin waves in local areas, it is used to study the thermal fluctuation of spin waves in this study. The BLS system uses a 532 nm Nd-YAG laser, and the laser beam can be focused on a circular spot 250 nm in diameter. An external field of 1,500 Oe is applied at a right angle to saturate the magnetization of the sample and maximize the Spin transfer torque (STT) effect.<sup>12,23,24</sup> Experiments are performed at room temperature.

## RESULTS AND DISCUSSION

Figure 2 shows the BLS spectrum intensity, reshaped by Lorentzian line fitting, in terms of the frequency, which is measured at the center of the Py<sub>1-x</sub>Co<sub>x</sub> layer with various DC currents of 3.5, 4, 4.5, 5, and 5.5 mA. The observed BLS spectrum represents the thermally excited quasi-uniform ferromagnetic resonance mode. The integral intensity of the BLS spectra thus indicates the total

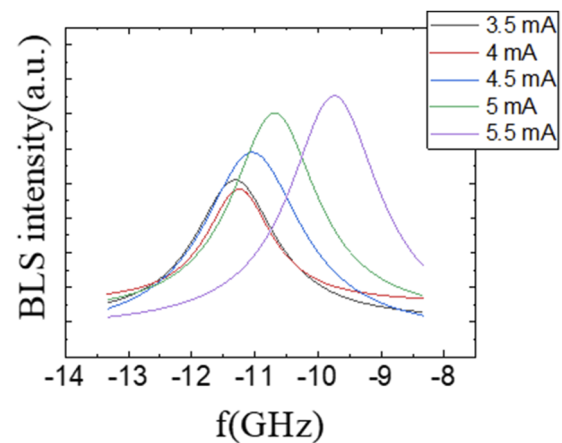


**FIG. 2.** BLS intensity spectra of Py<sub>79.05</sub>Co<sub>20.95</sub> nanowires with various applied DC currents of 3.5, 4.0, 4.5, 5.0 and 5.5 mA.

energy of magnetic fluctuations in the ferromagnetic layer.<sup>25</sup> The current flowing through the Pt layer would experience the spin-Hall effect and, as a result, transfer spin torque to the ferromagnetic layer. Thus, the enhanced magnetic fluctuation induced by the transferred spin torque is observed by the increase in BLS spectrum intensity, as shown in Fig. 2. The spectrum shape, which is broader than that of spin-torque ferromagnetic resonance (ST-FMR), is likely due to the contribution of nonuniform dynamic modes from spin-transfer torque.<sup>20</sup> In the magnetic system in Fig. 1, only magnetic fluctuations of spin waves, rather than auto-oscillations, are observed in the current values in Fig. 2 due to geometry limitations. The application of a larger current would induce another excitation mode, resulting in thermal mode hopping, which prevent the system from obtaining an auto-oscillation regime.<sup>7,26</sup>

In Fig. 2, we can infer the threshold current for auto-oscillations using the current dependence of BLS spectrum data.<sup>20</sup> According to

the theory of nonlinear auto-oscillations,<sup>13</sup> the inverse of the total fluctuation intensity below the threshold current regime should be linear to the current, and linear extrapolation can determine the threshold current of the system for auto-oscillations, i.e.,

$$\frac{1}{\bar{p}} \propto (I - I_{th})$$

where  $\bar{p}$  is the mean power of the spectrum and  $I$  and  $I_{th}$  are the bias and threshold current, respectively. Figure 3 shows the inverse of the integrated intensity of the BLS spectrum in terms of the bias current for the  $\text{Py}_{1-x}\text{Co}_x$  samples ( $x = 0, 0.1114, 0.2095, 0.2892$ , and  $0.4030$ ). The line is the linear extrapolation of the five data points. This shows that cosputtering  $\text{Py}_{1-x}\text{Co}_x$  ( $x \leq 0.2095$ ) noticeably reduces the threshold current, i.e., a 27.6% reduction in the threshold current for  $\text{Py}_{1-x}\text{Co}_x$  ( $x = 0.2095$ ) than for  $\text{Py}_{1-x}\text{Co}_x$  ( $x = 0$ ). A slight increase

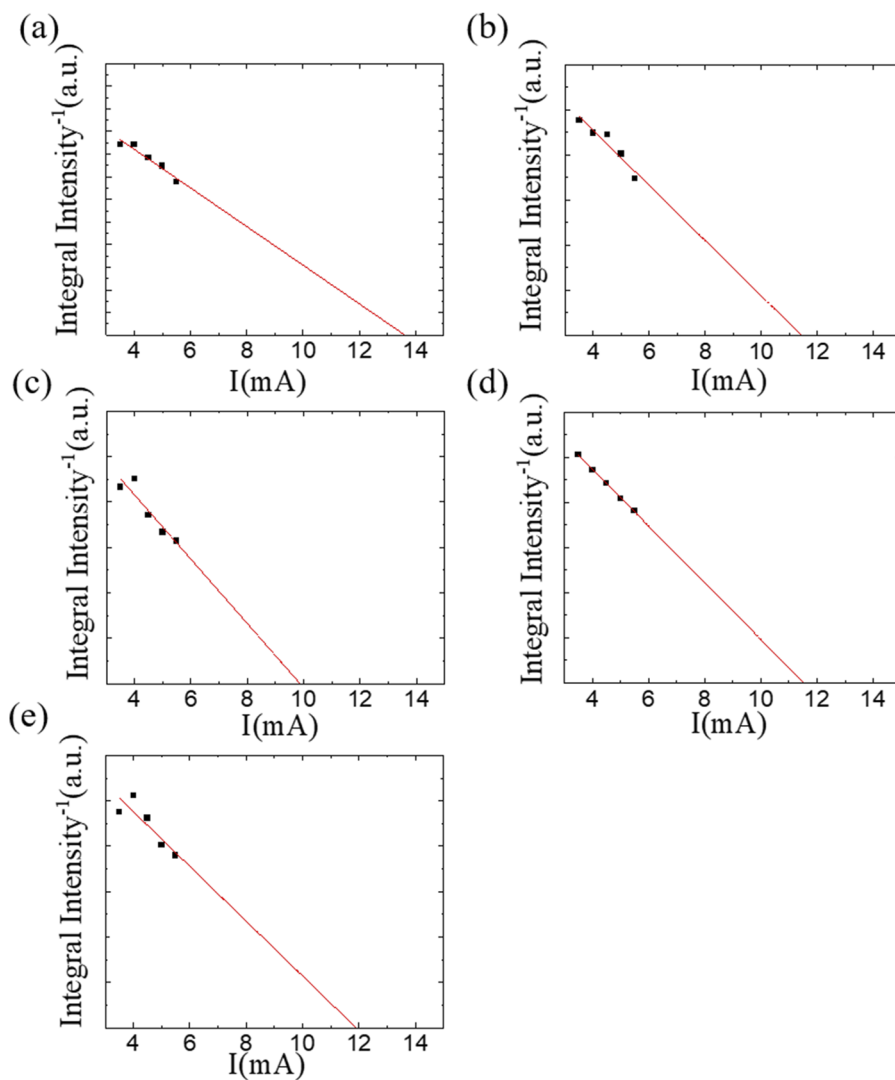


**FIG. 3.** Inverse of the integral BLS intensity of cosputtered samples of (a)  $\text{Py}_{1-x}\text{Co}_x$  ( $x = 0$ ), (b)  $\text{Py}_{1-x}\text{Co}_x$  ( $x = 0.1114$ ), (c)  $\text{Py}_{1-x}\text{Co}_x$  ( $x = 0.2095$ ), (d)  $\text{Py}_{1-x}\text{Co}_x$  ( $x = 0.2892$ ), and (e)  $\text{Py}_{1-x}\text{Co}_x$  ( $x = 0.4030$ ) in terms of applied DC current. The linear extrapolation of the data points yields a threshold current value for the auto-oscillation of the spin wave.

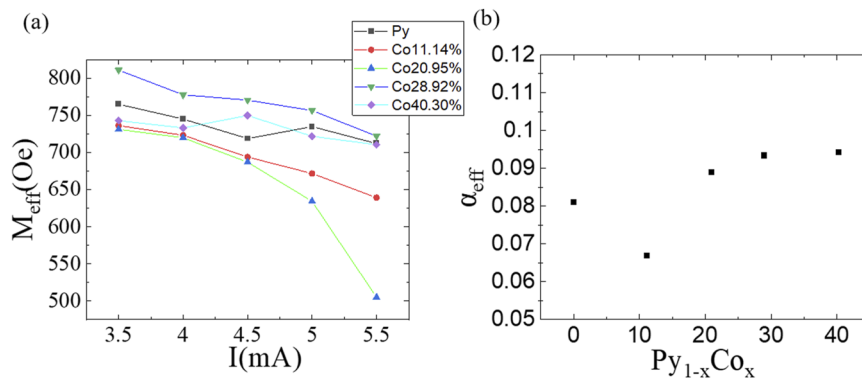


**FIG. 4.** (a) Effective magnetization in terms of applied DC current for the  $Py_{1-x}Co_x$  samples ( $x = 0, 0.1114, 0.2095, 0.2892, \text{ and } 0.4030$ ). (b) Effective Gilbert damping constant for the samples in (a) when a DC current of 5.5 mA is applied.

in the threshold value of  $Py_{1-x}Co_x$  ( $x > 0.2095$ ), which is still smaller than that of  $Py_{1-x}Co_x$  ( $x = 0$ ), is observed with increasing Co ratio.

Because the BLS signal is a result of quasi-ferromagnetic resonance due to the transferred spin torque, its spectrum shape is fitted with a Lorentzian approximation using the Kittel formula:

$$f_0 = \frac{\gamma}{2\pi} \sqrt{H(H + 4\pi M_{eff})},$$

where  $\gamma$  is the gyromagnetic ratio,  $f_0$  is the maximum peak frequency of the spectrum and  $M_{eff}$  is the effective magnetization. The field strength,  $H$ , is the sum of the applied field and induced field due to the current flowing in the Pt layer. We estimate that 80% of the current passes through the Pt layer because the resistivity of Pt is quite lower than that of  $Py_{1-x}Co_x$  and the Pt layer is two times thicker than the  $Py_{1-x}Co_x$  layer. From the fitting, as shown in Fig. 2, the effective magnetization is derived and plotted in terms of the applied current for the  $Py_{1-x}Co_x$  samples ( $x = 0, 0.1114, 0.2095, 0.2892, \text{ and } 0.4030$ ) in Fig. 4. A significant reduction in the  $M_{eff}$  of a sample of  $Py_{1-x}Co_x$  ( $x = 0.2095$ ) is observed compared to that of Py. In particular, the current dependence of reduction shows a clear non-linear effect, which is related to magnetic precession in  $Py_{1-x}Co_x$  ( $x = 0.2095$ ), as shown by the abrupt shift in frequency  $f_0$ . Nonlinearity is an essential characteristic of auto-oscillations that enhances the oscillation power and coherence between multiple oscillators using external microwaves and mutual synchronization.

The effective Gilbert damping constant can be determined using the Landau–Lifshitz–Gilbert equation combined with the demagnetization effect for the in-plane magnetization of a ferromagnetic film:

$$\alpha_{eff} = \frac{\Delta\omega}{2\gamma\sqrt{H(H + 4\pi M_{eff})}}$$

where  $\Delta\omega$  is the linewidth of the half maximum of the BLS spectrum. Figure 4(b) shows the effective damping constant for the  $Py_{1-x}Co_x$  samples ( $x = 0, 0.1114, 0.2095, 0.2892, \text{ and } 0.4030$ ) when the current is 5.5 mA. The  $\alpha_{eff}$  value of Py is estimated to be larger than the typical value ( $\approx 0.015$ ), obtained from ST-FMR measurements. This difference supports the scenario of spin wave excitation by spin-transfer torque because spin torque excites the nonuniform dynamic modes of the ferromagnetic layer, which, as a result, induces spectrum broadening. The  $\alpha_{eff}$  values of  $Py_{1-x}Co_x$  ( $x = 0.2095, 0.2892,$

and 0.4030) are found to be slightly larger than that of  $Py_{1-x}Co_x$  ( $x = 0$ ), while the  $\alpha_{eff}$  value of  $Py_{1-x}Co_x$  ( $x = 0.1114$ ) is quite smaller than the other values. The slight increase in the damping constant is consistent with the experimental study, which reports the damping constant of systems that are deposited by cosputtering Py with a transition metal.<sup>20</sup>

This observation shows that 20.95% cosputtering Co in the Py layer enhances the efficiency of spin torque for the auto-oscillation of spin waves and, on the other hand, induces almost no significant change in the damping constant. This result is consistent with a similar system that has a Co layer as the interface between the ferromagnetic layer and heavy-metal layer.<sup>21</sup> The study demonstrated that Co interface layer between FM and HM layer increase spin transparency. Also, Zhu *et al.* showed enhancement of spin transparency by inserting PtCo alloy spacers.<sup>27</sup> Considering Co has enhanced spin transparency as single interface layer and alloyed interface layer, we expect that threshold current for auto-oscillation is reduced due to enhancement of spin transparency by cosputtering Co and Py.

## CONCLUSION

We investigated the modulation of magnetic fluctuations in a stack of  $Py_{1-x}Co_x$  and Pt layers using the  $\mu$ -BLS spectrum when a  $Py_{1-x}Co_x$  layer is fabricated by Py-Co cosputtering. The data are used to estimate the threshold current for the auto-oscillations of the system. A significant reduction in the threshold current is achieved when the magnetic layer is fabricated by cosputtering 20.95% cobalt. In terms of applications, the results of this study provide a way to reduce the operation power and simplify the fabrication process of magnetic devices, utilizing auto-oscillations.

## SUPPLEMENTARY MATERIAL

See [supplementary material](#) which contains scanning electron microscopy (SEM) images and electron dispersion spectroscopy (EDS) images of the samples in study. The SEM and EDS mappings of Ni, Fe, and Co elements ensure the uniform distribution of the elements in samples.

## ACKNOWLEDGMENTS

This work was supported by a GIST Research Institute (GRI) grant funded by the GIST in 2022, by the Korea Institute of Industrial Technology (KITECH), and by a National Research Foundation of Korea (NRF) grant funded by the Ministry of Science and ICT (No. NRF-2022R1A2C1009516 and NRF-2018R1A2B6005183).

## AUTHOR DECLARATIONS

### Conflict of Interest

The authors have no conflicts to disclose.

### Author Contributions

**ByungRo Kim:** Conceptualization (equal); Formal analysis (equal); Validation (equal); Writing – original draft (equal). **S. Hwang:** Validation (equal). **Seungha Yoon:** Resources (equal); Supervision (equal). **S. H. Han:** Resources (equal); Writing – review & editing (equal). **B. K. Cho:** Resources (equal); Supervision (equal); Writing – review & editing (equal).

### DATA AVAILABILITY

The data that support the findings of this study are available from the corresponding author upon reasonable request.

## REFERENCES

- <sup>1</sup>B. Divinskiy, V. E. Demidov, S. Urazhdin, R. Freeman, A. B. Rinkevich, and S. O. Demokritov, *Adv. Mater.* **30**, e1802837 (2018).
- <sup>2</sup>M. Evelt *et al.*, *Phys. Rev. Appl.* **10**, 041002 (2018).
- <sup>3</sup>J. Wunderlich, B. Kaestner, J. Sinova, and T. Jungwirth, *Phys. Rev. Lett.* **94**, 047204 (2005).
- <sup>4</sup>J. Torrejon *et al.*, *Nature* **547**, 428 (2017).
- <sup>5</sup>V. E. Demidov, H. Ulrichs, S. V. Gurevich, S. O. Demokritov, V. S. Tiberkevich, A. N. Slavin, A. Zholud, and S. Urazhdin, *Nat. Commun.* **5**, 3179 (2014).
- <sup>6</sup>C. Leyder, M. Romanelli, J. P. Karr, E. Giacobino, T. C. H. Liew, M. M. Glazov, A. V. Kavokin, G. Malpuech, and A. Bramati, *Nat. Physics* **3**, 628 (2007).
- <sup>7</sup>V. E. Demidov, S. Urazhdin, A. Zholud, A. V. Sadovnikov, and S. O. Demokritov, *Appl. Phys. Lett.* **105**, 172410 (2014).
- <sup>8</sup>A. A. Awad, P. Dürrenfeld, A. Houshang, M. Dvornik, E. Iacocca, R. K. Dumas, and J. Åkerman, *Nat. Physics* **13**, 292 (2016).
- <sup>9</sup>C. Jin, J. Wang, W. Wang, C. Song, J. Wang, H. Xia, and Q. Liu, *Phys. Rev. Appl.* **9**, 044007 (2018).
- <sup>10</sup>M. Zahedinejad, A. A. Awad, S. Muralidhar, R. Khymyn, H. Fulara, H. Mazraati, M. Dvornik, and J. Åkerman, *Nat. Nanotechnol.* **15**, 47 (2020).
- <sup>11</sup>M. Haidar, A. A. Awad, M. Dvornik, R. Khymyn, A. Houshang, and J. Åkerman, *Nat. Commun.* **10**, 2362 (2019).
- <sup>12</sup>V. E. Demidov, S. Urazhdin, H. Ulrichs, V. Tiberkevich, A. Slavin, D. Baither, G. Schmitz, and S. O. Demokritov, *Nat. Mater.* **11**, 1028 (2012).
- <sup>13</sup>A. Slavin and V. Tiberkevich, *IEEE Trans. Magn.* **45**, 1875 (2009).
- <sup>14</sup>Y. Ou, D. C. Ralph, and R. A. Buhrman, *Phys. Rev. Lett.* **120**, 097203 (2018).
- <sup>15</sup>Y. Yin *et al.*, *Phys. Rev. B* **92**, 024427 (2015).
- <sup>16</sup>M. A. W. Schoen, D. Thonig, M. L. Schneider, T. J. Silva, H. T. Nembach, O. Eriksson, O. Karis, and J. M. Shaw, *Nat. Physics* **12**, 839 (2016).
- <sup>17</sup>Y. Fu *et al.*, *IEEE Trans. Magn.* **45**, 4004 (2009).
- <sup>18</sup>M.-H. Nguyen, M. Zhao, D. C. Ralph, and R. A. Buhrman, *Appl. Phys. Lett.* **108**, 242407 (2016).
- <sup>19</sup>H. Mazraati *et al.*, *Appl. Phys. Lett.* **109**, 242402 (2016).
- <sup>20</sup>H. Ulrichs, V. E. Demidov, S. O. Demokritov, W. L. Lim, J. Melander, N. Ebrahim-Zadeh, and S. Urazhdin, *Appl. Phys. Lett.* **102**, 132402 (2013).
- <sup>21</sup>W. Zhang, W. Han, X. Jiang, S.-H. Yang, and S. Parkin, *Nat. Physics* **11**, 496 (2015).
- <sup>22</sup>J. O. Rantschler, R. D. McMichael, A. Castillo, A. J. Shapiro, W. F. Egelhoff, B. B. Maranville, D. Pulugurtha, A. P. Chen, and L. M. Connors, *J. Appl. Phys.* **101**, 033911 (2007).
- <sup>23</sup>O. Mosendz, J. E. Pearson, F. Y. Fradin, G. E. Bauer, S. D. Bader, and A. Hoffmann, *Phys. Rev. Lett.* **104**, 046601 (2010).
- <sup>24</sup>M. Dvornik, A. A. Awad, and J. Åkerman, *Phys. Rev. Appl.* **9**, 014017 (2018).
- <sup>25</sup>S. O. Demokritov and V. E. Demidov, *IEEE Trans. Magn.* **44**, 6 (2008).
- <sup>26</sup>S. M. Rezende, F. M. de Aguiar, and A. Azevedo, *Phys. Rev. B* **73**, 094402 (2006).
- <sup>27</sup>L. Zhu, D. C. Ralph, and R. A. Buhrman, *Phys. Rev. B* **99**, 180404 (2019).